REGET/UFSM
Revista Eletrônica em Gestão, Educação e Tecnologia Ambiental

UFSM
REGET, Santa Maria v.24, e22 2020
DOI: https://doi.org/10.5902/2236117040800
ISSN 2236-1170

Environmental Tecnology
Submissão: 27/10/19 Aprovação: 21/11/19 Publicação: 15/04/20

Decolorization and degradation of methylene blue by photo−Fenton reaction under visible light using an iron−rich clay as catalyst: CCD−RSM design and LC−MS technique

Descoloração e degradação do azul de metileno por reação foto−Fenton sob luz visível utilizando uma argila rica em ferro como catalisador: planejamento DCCR e técnica CLEM

Bárbara Machado Zimmermann[I]
Enrique Chaves Peres[II]
Guilherme Luiz Dotto[III]
Edson Luiz Foletto[IV]

Abstract

In this work, an iron−rich bentonite was thermally modified at 200 °C and posteriorly used as a heterogeneous catalyst in the decolorization and degradation of methylene blue dye (MB) by photo−Fenton reaction under visible irradiation. The variables catalyst mass and pH were investigated in the reaction system, in order to detect the optimal decolorization conditions using the response surface methodology (RSM) coupled with Central Composite Design (CCD). Photodegradation of MB was analyzed by LC−MS technique. The results indicated that the optimal conditions to obtain 94% of MB decolorization efficiency were pH of 2.4 and catalyst mass of 0.02 g. It was also possible verify that the simultaneous combination of catalyst, hydrogen peroxide and visible light in the reaction medium was primordial for the increasing MB decolorization efficiency. MB degradation occurred partially at 180 min of photo−Fenton reaction, since the presence of dye in the solution was reduced, leading to its transformation into different intermediate products. Therefore, the catalyst used in this work has demonstrated a great potential for the degradation of cationic dye, allowing its use in advanced oxidation processes.

[I] Mestre em Engenharia Ambiental, Engenharia Sanitária e Ambiental, Universidade Federal de Santa Maria, Santa Maria, RS, Brasil
[II] Mestre em Engenharia Química, Engenharia Química, Universidade Federal de Santa Maria, Santa Maria, RS, Brasil
[III]Doutor em Engenharia e Ciência de Alimentos, Engenharia Química, Universidade Federal de Santa Maria, Santa Maria, RS, Brasil
[IV]Doutor em Engenharia Química, Engenharia Química, Universidade Federal de Santa Maria, Santa Maria, RS, Brasil

Keywords: Bentonite; Central composite design; Response surface methodology; Methylene blue; Photodegradation; Photo−Fenton

Resumo

Neste trabalho, uma bentonita rica em ferro foi modificada termicamente a 200 °C e posteriormente utilizada como catalisador heterogêneo na descoloração e degradação do corante azul de metileno (MB) pela reação foto−Fenton sob irradiação visível. As variáveis massa do catalisador e pH foram investigadas no sistema de reação para detectar as condições ideais de descoloração usando a metodologia da superfície de resposta (RSM) acoplada ao Delineamento Composto Central Rotacional (CCD). A fotodegradação do MB foi analisada pela técnica LC−MS. Os resultados indicaram que as condições ideais para obter 94% de eficiência de descoloração do MB foram pH de 2,4 e massa de catalisador de 0,02 g. Também foi possível verificar que a combinação simultânea de catalisador, peróxido de hidrogênio e luz visível no meio de reação foi primordial para o aumento da eficiência da descoloração. A degradação do MB ocorreu parcialmente aos 180 minutos de reação foto−Fenton, uma vez que a presença de corante na solução foi reduzida, levando à sua transformação em diferentes produtos intermediários. Portanto, o catalisador utilizado neste trabalho demonstrou um grande potencial para a degradação do corante catiônico, permitindo seu uso em processos avançados de oxidação.

Palavras−chave: Bentonita; Planejamento composto central; Superfície de resposta ; Azul de Metileno; Fotodegradação; Foto−Fenton

1 Introduction

Organic dyes are considered potential contaminants in natural waters due its high toxicity and recalcitrant character (NGUYEN and JUANG, 2013). The treatment of wastewaters containing these contaminants by conventional techniques may be inefficient, causing serious environmental problems (YONAR and KURT, 2017). Thus, novel methods are being employed to control the wastewater contamination (MESQUITA et al., 2016). In this context, advanced oxidation processes (AOPs) are attractive, since generate the hydroxyl radical (•OH), which is highly reactive and capable of degrading resistant organic pollutants (WU et al., 2016; FRAIESE et al., 2019; GHOSH et al., 2019; WAYHUNI et al., 2019). Among these, the Fenton process has the low−operating cost and low toxicity of the reagents (ÇINER, 2018). In Fenton processes, the •OH radicals are generated by the decomposition of hydrogen peroxide on the surface of heterogeneous catalyst under acidic media (GUPTA and GARG, 2018; WANG et al., 2014; MESQUITA et al., 2016; WANG et al., 2016). The •OH radical has a high oxidation potential (E°= + 2.8 V) and it is produced according to the following reactions (CASBEER et al., 2012):

$$Fe^{2+} + H_2O_2 \rightarrow Fe^{3+} + OH^- + {}^{\bullet}OH \quad (1)$$

$$Fe^{3+} + H_2O_2 \rightarrow Fe^{2+} + H^+ + {}^{\bullet}OOH \quad (2)$$

$$H_2O_2 + {}^{\bullet}OH \rightarrow H_2O + {}^{\bullet}OOH \quad (3)$$

$$Fe^{3+} + {}^{\bullet}OOH \rightarrow Fe^{2+} + H^+ + O_2 \quad (4)$$

The combination of Fenton reaction with light (called photo−Fenton reaction) produces a greater amount of •OH radicals (ALJUBOURY et al., 2017), according to the below reactions, and consequently, it accelerates the reaction rate (SEVERO et al., 2016).

$$Fe^{3+} + H_2O_2 + h\upsilon \rightarrow Fe^{2+} + {}^{\bullet}OOH + H^{+} \quad (5)$$

$$Fe^{2+} + H_2O_2 + h\upsilon \rightarrow Fe^{3+} + {}^{\bullet}OH + OH^{-} \quad (6)$$

Methylene blue (MB) has been chosen as model substrate in this work because this cationic dye has been widely used in textile, pharmaceutical, leather, plastics, food and paper industries, and also, in the medicine field (PANG et al., 2017; UYAR et al., 2016; WU et al., 2016). However, this dye is responsible for causing harmful effects to human health and environment (ANFAR et al., 2017). It can cause eye permanent injury of humans and animals, nausea, diarrhea, vomiting, respiratory distress and mental confusion (FAYAZI et al., 2016; WU et al., 2016).

Bentonite clay is ubiquitous presence in most soils, and can present iron in its composition, being that quartz and feldspar are frequent (ANDRINI et al., 2017; BELBACHIR and MAKHOUKHI, 2017). This clay can exhibit excellent properties, as large specific surface area, high cation exchange capacity (CEC) and low permeability, which gives it a wide application as adsorbents and catalysts (BELBACHIR and MAKHOUKHI, 2017; ZONG et al., 2015). The work of Zimmermann et al. (2019) showed an increase of the specific surface area of these clays when subjected to thermal treatment at 200 °C.

In this work, thermally treated iron−rich clay was evaluated as heterogeneous catalyst for the decolorization and degradation of methylene blue (MB) by photo−Fenton under visible light. Effects of variables such as pH and catalyst mass on the decolorization of MB were studied using Response Surface Methodology (RSM) based on Central Composite Design (CCD) 2^K. The evaluation of the photodegradation was by LC−MS under the same

optimal condition found on the experimental design. The characterization of the catalyst was investigated by techniques of XRD, BET, FTIR, XRF and SEM.

2 Material and methods

2.1 Thermal treatment of bentonite

A sample (5 g) of comminuted raw bentonite from Lages city (Santa Catarina State, Brazil) was exposed at 200 °C for 24 h in air atmosphere.

2.2 Characterization techniques

X−ray diffraction (XRD) analysis of sample was carried out using a Rigaku−Miniflex 300 diffractometer, operated with CuKα (λ= 1.54051 Å), 30 kV, 10 mA, step size 0.03°, acquisition time of 0.9 s by step and scan range of 2θ= 5 to 30°. N_2 adsorption−desorption isotherm of the catalyst was obtained by Micromeritics ASAP 2020 equipment at 77 K. The specific surface area and pore−size distribution of treated bentonite was analyzed by Brunauer–Emmett–Teller (BET) and Barrett–Joyner–Halenda (BJH) methods. Fourier transform infrared (FTIR) spectroscopy was performed by the Shimadzu−IR Prestige 21 equipment. Morphological characteristics of the sample were examined using scanning electron microscopy (SEM; Jeol, JSM 6010LV). The chemical composition of the sample was obtained by X−ray fluorescence spectrometry (XRF). X−ray fluorescence measurements were carried out in a spectrometer (Bruker, S8 Tiger) with a Pd X−ray tube (maximum power 50 W). Bentonite (50% wt.) was mixed with KBr (50% wt.) to form a pellet and this pellet was submitted to the analysis. Blank test with only KBr was performed. The spectrum evaluation was performed by Spectra EDX (Bruker AXS) software.

2.3 Reaction apparatus, experimental essays and analytical procedures

The experiments were conducted in a routine manner at ambient temperature (25 °C) in batch mode. The solutions (V = 100 mL) of Methylene blue (C_0 = 50 mg L^{-1}) were magnetically stirred in the dark for 150 min until the establishment of adsorption equilibrium between the catalyst and the dye solution. After, H_2O_2 was added and the lamp

(*spiral* compact *fluorescent,* Empalux/85 W) was turned on, keeping the solution under stirring for 180 min. Finally, these samples were centrifuged and then analyzed using UV–vis spectrophotometry. The photodegradation was evaluated to the optimum point of the experimental design. The samples were centrifuged, filtered by syringe filter and had pH adjusted to basic with 6 mol L^{-1} NaOH solution, to interrupt the reaction.

The decolorization of Methylene Blue ($C_{16}H_{18}N_3SCl$; 319.96 g mol^{-1}) was analyzed in terms of absorbance reduction of the dye at λ_{max} = 664 nm using an UV−visible spectrophotometer (UVmini−1240, Shimadzu). The percentage of decolorization efficiency (*DE*, %) was calculated through the Eq. (7):

$$DE, \% = \left(1 - \frac{C}{Co}\right) 100 \quad (7)$$

where: C_0 is the initial concentration of MB and *C* is the concentration at a given time.

The photodegradation was determined by Liquid Chromatography coupled to Mass Spectrometry (LC−MS) using an electrospray ionization mass spectrometer (Agilent Technologies − 6460 Triple Quadrupole LC/MS) in order to verify the fragmentation of dye molecules. The methodology of equipment operation and analytical conditions are described by Zimmermann et al. (2019).

2.4 Experimental design

Two factors were chosen to observe its influence in the photo−Fenton process (pH and catalyst mass). The decolorization efficiency (*DE*,%) was chosen as response factor. A 2^k CCD was done, consisting of eleven experiments (in the case of k = 2 variables more 3 at central points). These variables were codified in five levels (-α, -1, 0, +1, +α), where α are the extreme points with value of 1.41. The catalyst mass studied on experimental design varied from 0.01 to 0.02 g, and the pH, from 2.2 to 2.8. The initial concentrations of H_2O_2 and MB were, respectively, 7.2×10^{-3} mol L^{-1} and 50 mg L^{-1} for all experimental assays.

The pH values were stipulated according to the literature, i.e, between 2 and 3 (WANG et al., 2014), since that at a pH higher than 3 or below 2, the production of •OH radicals is reduced (GUPTA and GARG, 2018; KWON et al., 1999; WANG et al., 2016). The equilibrium time was chosen from preliminary tests and the dye concentration, according to the literature (MESQUITA et al., 2016; REDDY et al., 2013; ZHOU et al., 2015). The H_2O_2 concentration was calculated according to reaction stoichiometry (GÓMEZ et al., 2016), since at this way, the total conversion of MB to CO_2 and H_2O can occur. Table 1 demonstrates the values of coded variables (pH and catalyst mass).

Table 1 – Experimental range and levels of process variables.

Independent variables	Coded variables	Levels				
		-1.41	**-1**	**0**	**1**	**1.41**
Catalyst mass (g)	A	0.01	0.0115	0.015	0.0185	0.02
pH	B	2.2	2.29	2.5	2.71	2.8

3 Results and discussion

3.1 Catalyst characterization

X–ray diffraction pattern (Fig. 1a) of catalyst sample shows a peak of the smectite at 2θ = 5.6° and presence of quartz at 2θ = 26°. The thermally treated bentonite presented a surface area of 100 $m^2\ g^{-1}$. According to IUPAC classification, the isotherms shown in Fig. 1 (b) are of type IV, representing a predominantly mesoporous structure, confirmed by the pore–size distribution (THOMMES et al., 2015). FTIR spectrum shown in Fig. 1c exhibits absorption bands attributed to the stretching and bending vibrations of functional groups of bentonite clay. These bands are located at 3450, 1650, 1030, 915, 795 and 520 cm^{-1}. At 3450 and 1650 cm^{-1}, stretching and bending vibrations of the –OH groups can be observed. The Si–O–Si bond stretching in the tetrahedral sheet of the material can be verified in 1030 cm^{-1}. At 915 cm^{-1}, the Al–OH group can be also observed. According to Zimmermann et al. (2019), bands at 795 and 520 cm^{-1} are relative to the bending of Si–O (quartz) bonds and Si–O–Al bonds, respectively. Fig. 1d shows the SEM image of treated bentonite sample, whose particles present irregular sizes and shapes. From XRF analysis, the chemical

composition (wt.%) of sample was: 55.56 (SiO_2), 25.05 (Al_2O_3), 9.75 (Fe_2O_3), 1.37 (MgO), 1.55 (P_2O_5), 1.08 (TiO_2), 0.33 (K_2O), 0.11 (Na_2O), 0.07 (CaO), 0.02 (MnO), and 5.11 (loss on ignition: sample calcined at 900 °C). Therefore, the sample has a considerable iron content expressed in terms of Fe_2O_3 (about 10 wt.%).

Figure 1 − (a) XRD, (b) N_2 adsorption−desorption isotherms and pore−size distribution (inset), (c) FTIR spectrum and (d) SEM image of the catalyst particles.

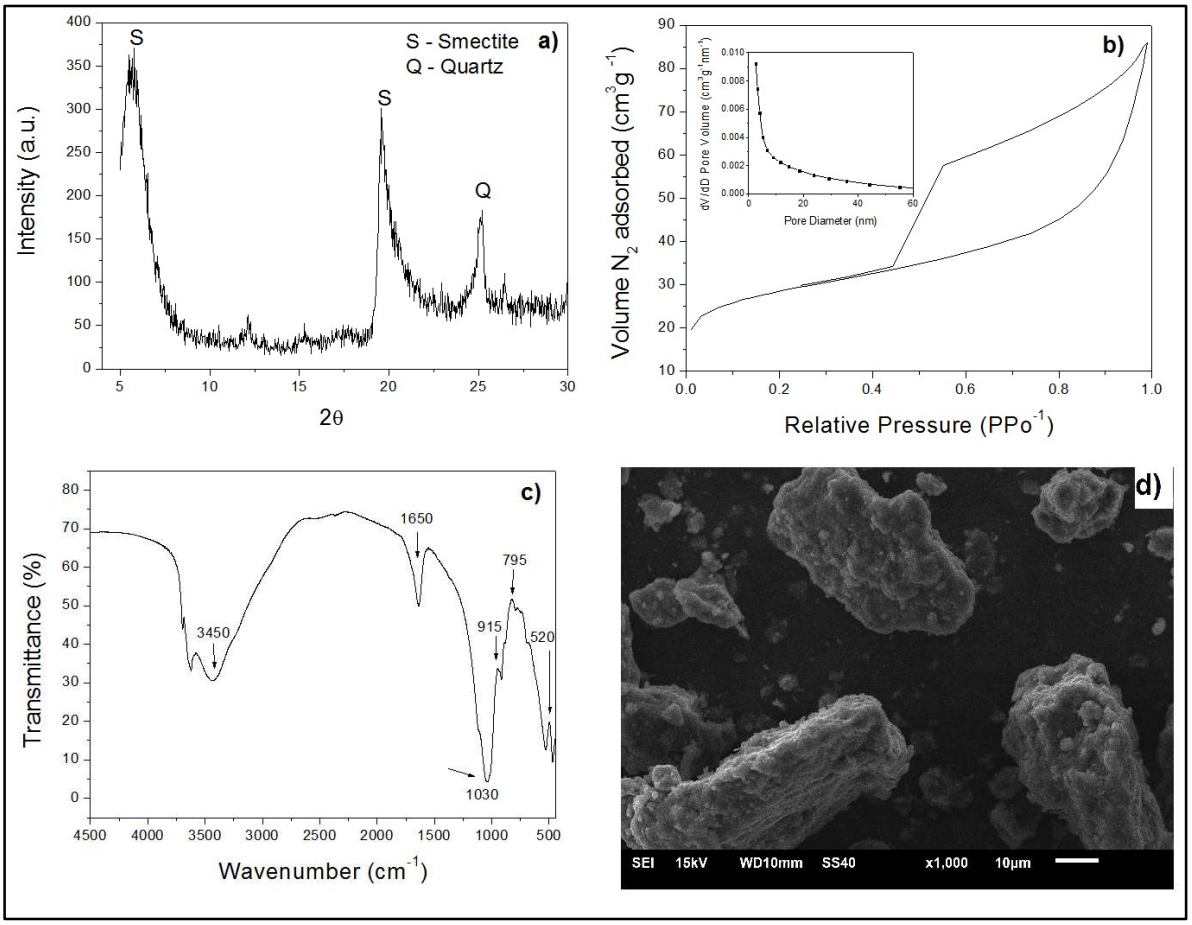

3.2 Decolorization by photo−Fenton

The experimental and predicted values on the CCD for the decolorization efficiency are provided in Table 2, with a confidence level of 90 %. The observed values ranged between 61–92% and are in good agreement with the predicted values (58–93%), as shown in Fig. 2. The test 9 obtained a better decolorization result, because the catalyst mass used was the highest of the others studied, causing the increase of the contact between the catalyst and

the dye for the occurrence of the photo−Fenton reaction. Moreover, Fig. 2 shows any tendency on data acquisition.

Pareto Chart demonstrated in Fig. 3 shows that all variables, with exception of the interaction 1Lby2L, were significant. The values estimated for the isolated effects show the strong linear influence of catalyst mass (A) (16.8) in relation to pH (B) linear influence (−3.15). The positive signal value of catalyst mass represents that increases in this factor cause elevation on decolorization efficiency, but, the negative value of quadratic term represents the presence of equilibrium in a specific catalyst concentration (0.02 g). In relation to pH, the negative values of linear and quadratic effects, with low values in relation the catalyst mass, meaning that the pH has a negative effect with a lower contribution in decolorization efficiency. Equation 8 represents the model adjusted to the data, which was obtained through the CCD methodology for the decolorization efficiency (*DE*) of methylene blue.

$$DE(\%) = 83.34 + 12.34\,A - 3.744\,A^2 - 2{,}321\,B - 3{,}241\,B^2 \quad (8)$$

where, *A* represent the catalyst mass and *B* represent the solution pH.

Table 1 − Experimental design matrix, experimental runs, and predicted values of efficiency decolorization of MB by photo−Fenton process.

Run	**Coded variables**		**Dependent variable**	
			Decolorization efficiency (%)	
	A	**B**	**Observed values**	**Predicted values**
1	-1	-1	62	66
2	1	-1	91	91
3	-1	1	62	62
4	1	1	88	86
5	0	0	81	83
6	0	0	84	83

7	0	0	85	83
8	-1.41	0	61	58
9	1.41	0	92	93
10	0	-1.41	83	80
11	0	1.41	72	74

Figure 1 − Predicted versus observed values for the MB decolorization efficiency by photo−Fenton process as a function of pH and catalyst mass.

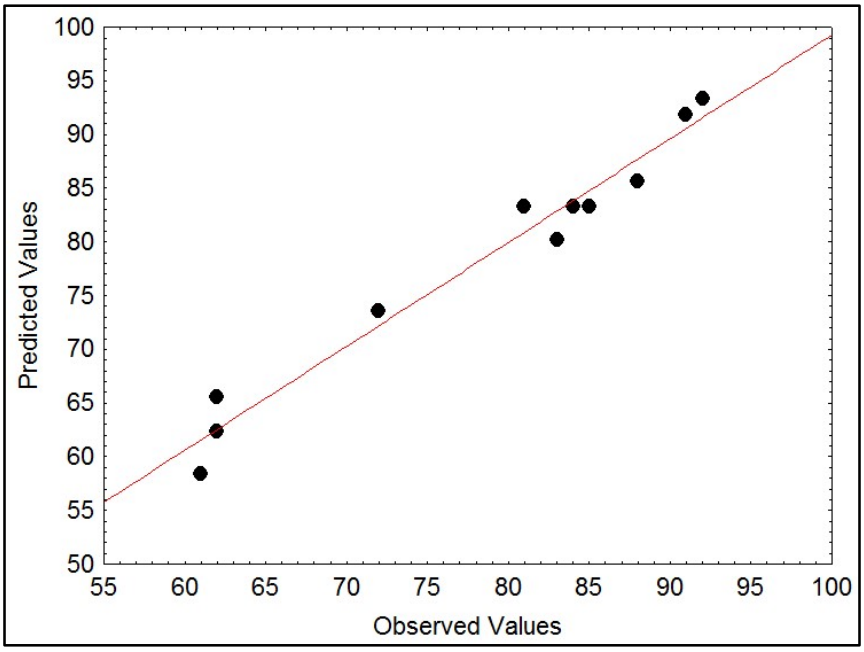

The correlation *AB* between mass catalyst and pH was not significant, as shown in the Pareto chart. The values of coefficient of determination (R^2) and adjusted determination coefficient (R^2_{adj}) were 0.9655 and 0.9453, respectively.

(Continue...)

Figure 2 – Pareto Chart showing the influence of catalyst mass and pH (linear (L) and quadratic (Q)) on the MB decolorization efficiency

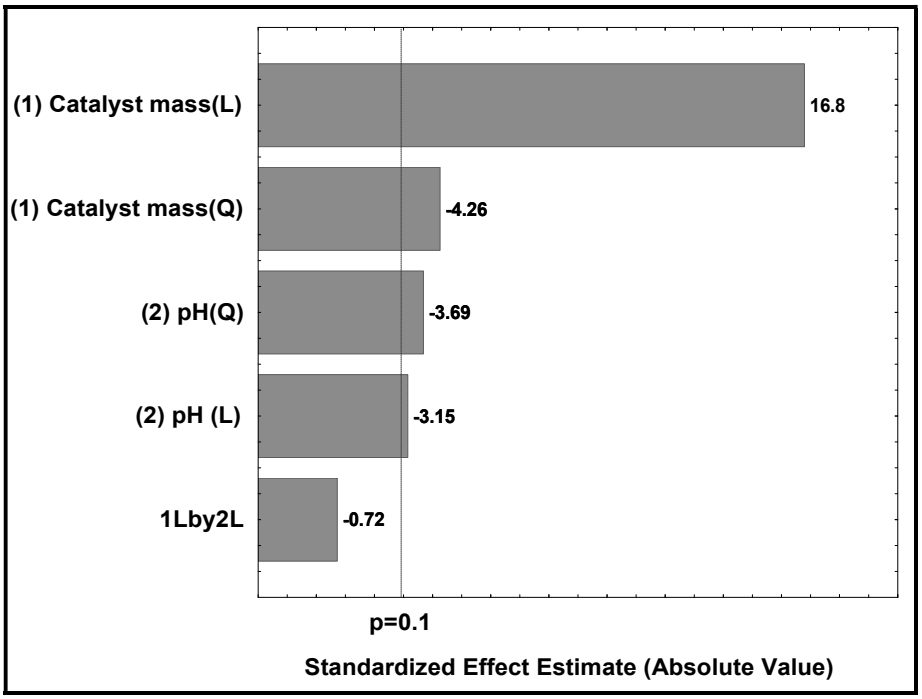

Another important factor to verify the viability of the model was to calculate the F value through the ANOVA (Analysis of Variance) method. ANOVA results represent the significance and contribution of each process parameter evaluated, where *p* values for each linear, interaction or quadratic model components were compared.

Table 2 – ANOVA results for CCD design.

	Sum of squares (SS)	**Degree of freedom (DF)**	**Mean square (MS)**	***p*–value**	**F_{model}**
A (L)	1222	1	1222	0.004	43.10
A (Q)	78.54	1	78.54	0.051	
B (L)	42.96	1	42.96	0.088	
B (Q)	58.85	1	58.85	0.066	
Residual SS	48.79	6	8.13		
Total SS	1420.18	10			

The results presented in Table 3 indicate that the most important term is catalyst mass linear (A(L)). All parameters present a *p*−value minor than 0.1, with a significance level of 10%, discarding A in relation B with the Pareto Chart, to calculating F−value. Moreover, the signs of these terms can be provide physical significance to the obtained results. For instance, larger A (catalyst mass) values would also result in a higher decolorization efficiency, demonstrating the importance on the photo−Fenton reaction. The calculated F was equivalent to 43.10 and the F tabulated to 3.18, confirming that the model is predictive and significant.

Thus, with the statistically validated model, it was possible to construct the response surface for the decolorization efficiency of methylene blue dye. The response surface (Fig. 4) described by Eq. (8) suggests that higher percentages of decolorization efficiency can be obtained using pH = 2.4 and catalyst mass = 0.02 g. The major effect was the catalyst mass, where the best result of decolorization was on maximum catalyst dosage, proving the positive effect of linear term. Therefore, increasing catalyst mass causes greater dye degradation. In the curve, the pH effect is very small, with negative signal effect to influence the decolorization efficiency, in view of the fact that the best results are obtained on lower values of pH.

Figure 3 − Response surface for the MB decolorization efficiency as a function of catalyst mass and pH

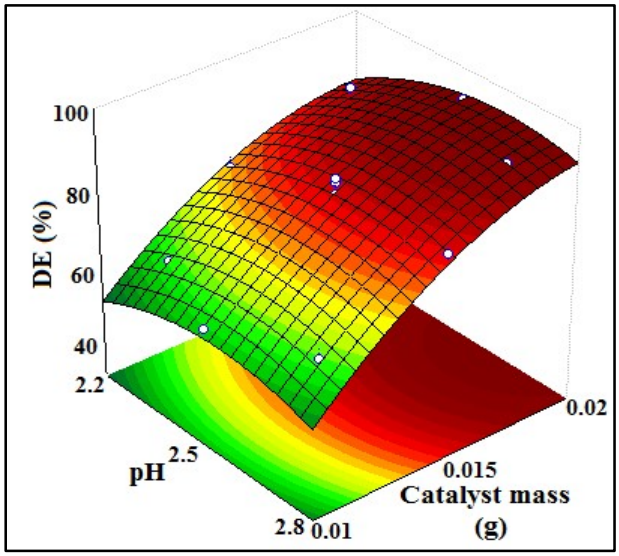

Optimized experiments were realized to verify the effect of absence of catalyst, H_2O_2 concentration and absence of visible light on the MB decolorization. The results are shown in Table 4. In absence of catalyst (H_2O_2 /visible light system), low decolorization of 5.3 % was observed. Moreover, other parameters as H_2O_2 concentration and visible light showed a great impact on decolorization efficiency, 37% and 36%, respectively. Therefore, higher decolorization efficiency of MB dye was observed from the combination of the hydrogen peroxide, catalyst and light source (photo−Fenton system). This same result was obtained in the statistic model (Eq. 8). Therefore, the experimental data prove that the decolorization efficiency obtained by the model is similar to the generated on the statistical analysis.

Table 3 − Influence of different conditions on the decolorization process.

Parameters	**Decolorization efficiency (%)**
Photo−Fenton	93.9
Catalyst + visible light	37
Fenton (H_2O_2 + catalyst)	36
H_2O_2 + visible light	5.3

3.3 Photodegradation

The mass spectrum showed in Fig. 5 presents the possible intermediate structures formed during the photodegradation of the Methylene Blue dye. From Fig. 5, the peak in *m/z* = 284 corresponds to molecule of MB dye. However, the chlorine mass of the structure was not accounted in the spectrum due to the fact that it rapidly ionizes in the solution. The reduction of the presence of the contaminant and its oxidation can be confirmed because the intensity of this signal reduced throughout the reaction and new intermediates were formed.

(Continue...)

Figure 4 − Possible intermediates formed during the photo−Fenton reaction of MB under visible light using an iron−rich clay as catalyst.

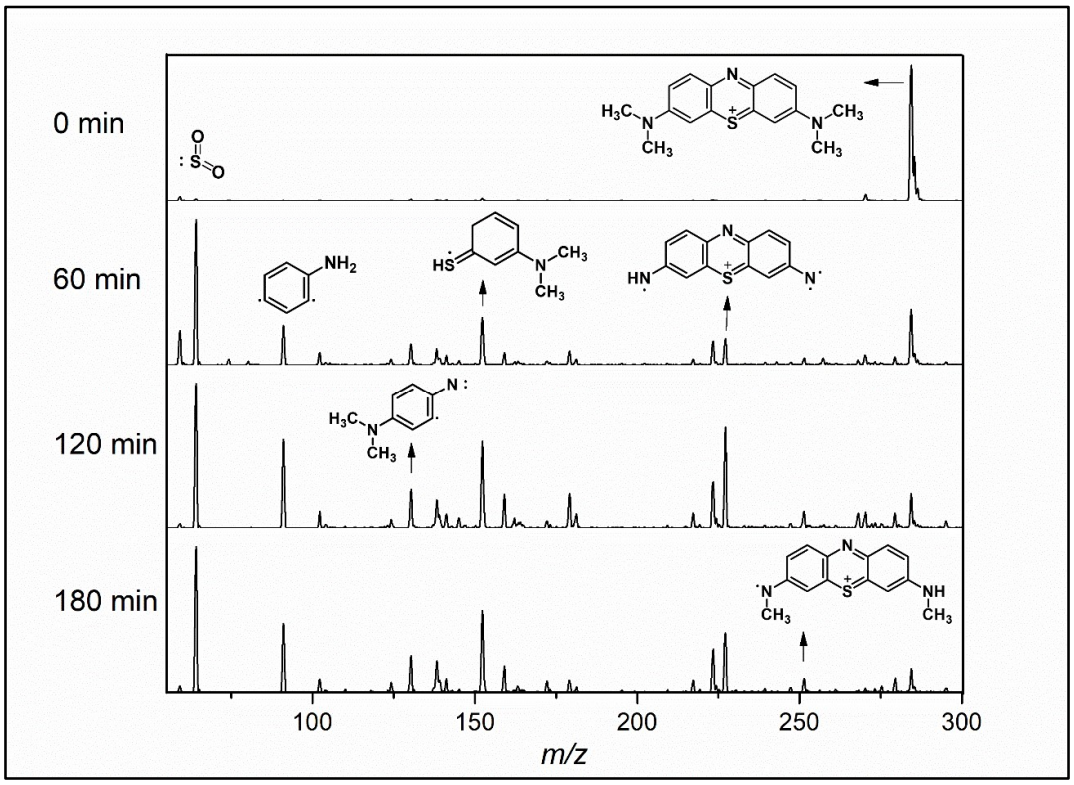

Fragmentation of the molecule may have resulted in the formation of possible intermediates represented by mass peaks *m/z* = 252, 227, 152, 130, 90 and 64. At *m/z* = 252 and 227, the breakage of N−CH_3 bonds was detected, while the central ring opening generated the peaks at 152 and 130. In the peak *m/z* = 90 (phenylamine), there was loss of the −N−dimethyl structure, which was attached to the aromatic ring. Finally, mass 64 was attributed to the formation of sulfur dioxide. Thus, under the conditions studied, it can affirm that the partial degradation of the Methylene Blue occurred.

4 Conclusions

It was studied the decolorization and degradation of methylene blue by photo−Fenton reaction under visible light using an iron−rich clay as catalyst. CCD−RSM design and LC−MS techniques were used. Through the CCD, it was possible to optimize the operational conditions, which were pH of 2.4 and catalyst mass of 0.02 g. Under these conditions at 180

min of reaction, 94% of decolorization efficiency was obtained. The combination of catalyst, hydrogen peroxide and visible light (photo−Fenton reaction) was paramount for increased degradation. The study by mass spectrometry confirmed that the mechanism of degradation occurred via the photo−Fenton system. Thus, under the conditions studied, a remarkable capacity of iron−rich bentonite used as a heterogeneous photo−Fenton catalyst for the decolorization and degradation of MB dye was observed.

Acknowledgment

The CAPES for the financial incentive.

References

ALJUBOURY, D.A.D.A.; PALANIANDY, P.; ABDUL AZIZ, H.B.; FEROZ, S. Degradation of total organic carbon (TOC) and chemical oxygen demand (COD) in petroleum wastewater by solar photo−Fenton process. **Global NEST Journal**, v. 19, p. 430–438, 2017.

ANDRINI, L.; TOJA, R.M.; GAUNA, M.R.; CONCONI, M.S.; REQUEJO, F.G.; RENDTORFF, N.M. Extended and local structural characterization of a natural and 800 °C fired Na−montmorillonite–Patagonian bentonite by XRD and Al/Si XANES. **Applied Clay Science**, v. 137, p. 233–240, 2017.

ANFAR, Z.; HAOUTI, R.E.; LHANAFI, S.; BENAFQIR, M.; AZOUGARH, Y.; EL ALEM, N. Treated digested residue during anaerobic co−digestion of agri−food organic waste: Methylene blue adsorption, mechanism and CCD−RSM design. **Journal of Environmental Chemical Engineering**, v. 5, p. 5857–5867, 2017.

BELBACHIR, I.; MAKHOUKHI, B. Adsorption of Bezathren dyes onto sodic bentonite from aqueous solutions. **Journal of the Taiwan Institute Chemical Engineers**, v. 75, p. 105–111, 2017.

CASBEER, E.; SHARMA, V.K.; LI, X. Synthesis and photocatalytic activity of ferrites under visible light: A review. **Separation and Purification Technology**, v. 87, p. 1–14, 2012.

ÇINER F. Application of Fenton reagent and adsorption as advanced treatment processes for removal of Maxilon Red GRL. **Global NEST Journal**, v. 20, p. 1–6, 2018.

FAYAZI, M.; TAHER, M.A.; AFZALI, D.; MOSTAFAVI, A. Enhanced Fenton−like degradation of methylene blue by magnetically activated carbon/hydrogen peroxide with hydroxylamine as Fenton enhancer. **Journal of Molecular Liquids**, v. 216, p. 781–787, 2016.

FRAIESE, A.; NADDEO, V.; UYGUNER−DEMIREL, C.S.; PRADO, M.; CESARO, A.; ZARRA, T.; LIU, H.; BELGIORNO, V.; BALLESTEROS JR. F. Removal of emerging contaminants in wastewater by sonolysis photocatalysis and ozonation. **Global NEST Journal**, v. 21, p. 98–105, 2019.

GHOSH, P.; GHIME, D.; GORU, P.; OJHA, S. Oxidative decolorization of a malachite green oxalate dye through the photochemical advanced oxidation processes. **Global NEST Journal**, v. 21, p. 195−203, 2019.

GÓMEZ, M.; MURCIA, M.D.; GOMEZ, E.; ORTEGA, S.; SANCHEZ, A.; THAIKOVSKAYA, O.; BRIANTCEVA, N. Modelling and experimental checking of the influence of substrate concentration on the first order kinetic constant in photo−processes. **Journal of Environmental Management**, v. 183, p. 818−825, 2016.

GUPTA, A.; GARG, A. Degradation of ciprofloxacin using Fenton's oxidation: effect of operating parameters, identification of oxidized by−products and toxicity assessment. **Chemosphere**, v. 193, p. 1181−1188, 2018.

KWON, B.G.; LEE, D.S.; KANG, N.; YOON, J. Characteristics of p−chlorophenol oxidation by Fenton's reagent. **Water Research**, v. 33, p. 2110−2118, 1999.

MESQUITA, A.M.; GUIMARÃES, I.R.; CASTRO, G.M.M.; GONÇALVES, M.A.; RAMALHO, T.C.; GUERREIRO, M.C. Boron as a promoter in the goethite (α−FeOOH) phase: organic compound degradation by Fenton reaction. **Applied Catalysis B: Environmental**, v. 192, p. 286–295, 2016.

NGUYEN, T.A.; JUANG, R.S. Treatment of waters and wastewaters containing sulfur dyes: a review. **Chemical Engineering Science**, v. 219, p. 109–117, 2013.

PANG, J.; FU, F.; DING, Z.; LU, J.; LI, N.; TANG, B. Adsorption behaviors of methylene blue from aqueous solution on mesoporous birnessite. **Journal of the Taiwan Institute Chemical Engineers**, v. 77, p. 168–176, 2017.

REDDY, P.M.K.; RAJU, B.R.; KARUPPIAH, J.; REDDY, E.L.; SUBRAHMANYAM, C. Degradation and mineralization of methylene blue by dielectric barrier discharge non−thermal plasma reactor. **Chemical Engineering Journal**, v. 217, p. 41–47, 2013.

SEVERO, E.C.; ANCHIETA, C.G.; FOLETTO, V.S.; KUHN, R.C.; COLLAZZO, G.C.; MAZUTTI, M.A.; FOLETTO E.L. Degradation of Amaranth azo dye in water by heterogeneous photo−Fenton process using $FeWO_4$ catalyst prepared by microwave irradiation. **Water Science & Technology**, n. 1, v. 73, p. 88–94, 2016.

THOMMES, M.; KANEKO, K.; NEIMARK, A.V.; OLIVIER, J.P.; RODRIGUEZ−REINOSO, F.; ROUQUEROL J.; SING K.S.W. Physisorption of gases, with special reference to the evaluation

of surface area and pore size distribution (IUPAC Technical Report). **Pure and Applied Chemistry**, p. 1−19, 2015.

UYAR, G.; KAYGUSUZ, H.; ERIM, F.B. Methylene blue removal by alginate–clay quasi−cryogel beads. **Reactive and Functional Polymers**, v. 106, p. 1–7, 2016.

WAYHUNI, E.T.; SISWANTA, D.; KUNARTI, E.S.; SUPRABA, D.; BUDIRAHARJO, S. Removal of Pb (II) ions in the aqueous solution by photo−Fenton method. **Global NEST Journal**, v. 21, p. 180–186, 2019.

WANG, Y.; ZHAO, H.; LI, M.; FAN, J.; ZHAO, G. Magnetic ordered mesoporous copper ferrite as a heterogeneous Fenton catalyst for the degradation of imidacloprid. **Applied Catalysis B: Environmental**, v. 147, p. 534– 545, 2014.

WANG, N.; ZHENG, T.; ZHANG, G.; WANG, P. A review on Fenton−like processes for organic wastewater treatment. **Journal of Environmental Chemical Engineering**, v. 4, p. 762–787, 2016.

WU, Q.; ZHANG, H.; ZHOU, L.; BAO, C.; ZHU, H.; ZHANG, Y. Synthesis and application of rGO/$CoFe_2O_4$ composite for catalytic degradation of methylene blue on heterogeneous Fenton−like oxidation. **Journal of the Taiwan Institute of Chemical Engineers**, v. 67, p. 484–494, 2016.

YONAR, T.; KURT A. Treatability studies of hospital wastewaters with AOPs by Taguchi´s experimental design. **Global NEST Journal**, v. 19, p. 505−510, 2017.

ZIMMERMANN, B.M.; SILVESTRI, S.; LEICHTWEIS, J.; DOTTO, G.L.; MALLMANN, E.S.; FOLETTO E.L. Effect of thermal treatment on the catalytic activity of a Fe−rich bentonite for the photo−Fenton reaction. **Cerâmica**, v. 65, p. 147−152, 2019.

ZHOU, G.; FANG, F.; CHEN, Z.; HE, Y.; SUN, H.; SHI, H. Facile synthesis of paper mill sludge−derived heterogeneous catalyst for the Fenton−like degradation of methylene blue. **Catalysis Communications**, v. 62, p. 71–74, 2015.

ZONG, P.; WU, X.; GOU, J.; LEI, X.; LIU, D.; DENG, H. Immobilization and recovery of uranium (VI) using Na−bentonite from aqueous medium: equilibrium, kinetics and thermodynamics studies. **Journal of Molecular Liquids**, v. 209, p. 358–36, 2015.